Monatshefte für Chemie 136, 677–692 (2005)
DOI 10.1007/s00706-004-0250-2

**Monatshefte für Chemie**
**Chemical Monthly**
Printed in Austria

# Mononuclear and Binuclear Fe(III), Co(II), Ni(II), and Cu(II) Complexes of 3,4′-Dihydroxyazobenzene-3′,4-dicarboxylic Acid and 3-Carboxy-4-hydroxyphenylazo-3-carboxy-4-hydroxynaphthalene

**Kamal Y. El-Baradie***

Chemistry Department, Faculty of Science, Tanta University, Tanta, Egypt

Received June 18, 2004; accepted (revised) August 3, 2004
Published online February 4, 2005 

**Summary.** Fe(III), Co(II), Ni(II), and Cu(II) complexes of the title azodyes have been synthesized and characterized by elemental analysis, molar conductance, TGA, DTA, magnetic susceptibility measurements, IR, electronic and ESR spectral studies. The spectral studies suggest an octahedral geometry for Fe(III) and Co(II) complexes but a square planar geometry for Ni(II) and Cu(II) complexes. The kinetics of the catalysed oxidation of *N*,*N*,*N*′,*N*′-tetramethyl-*p*-phenylenediamine dihydrochloride (*TMPPD*) with mononuclear and binuclear copper complexes were studied to check the activity of these copper complexes in oxidizing organic amines. The electrochemical behaviour of the metal complexes was studied using DC polarography and cyclic voltammetry. Antimicrobial activity of the azo compounds and its complexes have been tested against different microorganisms.

**Keywords.** Azodyes; Complexes; Fe(III); Co(II); Ni(II); Cu(II); Spectra; Biological activity.

## Introduction

Azo compounds have played an important role in the development of coordination chemistry as they readily form stable complexes with most transition metal ions. Metal complexes with hydroxy- and carboxyphenylazo compounds were of interest to many authors. Several complexes with metal ions from the first transition series have been prepared and characterized using elemental analysis, *IR* spectra, magnetic moment, electronic spectra, and conductometric measurements [1–3].

Azo compounds containing a heterocyclic moiety were found to form readily complexes with transition metal ions. Pyrazolone azodyes have drawn the attention of some research concerning their importance in dye industry as well as analytical

* E-mail: kyelbaradie@hotmail.com

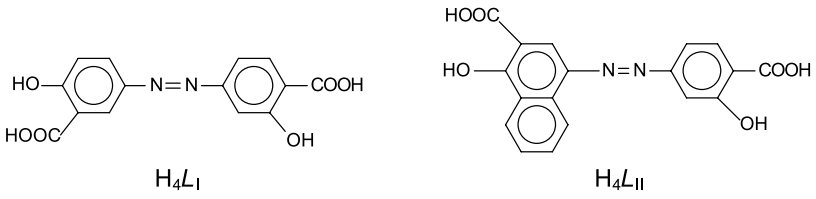


$H_4L_I$ $H_4L_{II}$

**Fig. 1.** Structures of azodyes

application [4]. Their excellent ability to form metal complexes attracted the attention of coordination chemists to study their reaction with transition metal ions [5–7].

The coordination abilities of 2-(arylazo)imidazole [8, 9], 2-(napthylazo)imidazole [10], benzimidazols [11], and arylazopyrimidine [12] have been used successfully to synthesis various metal complexes.

Metal chelates of some transition metal ions with chromone azodyes were synthesized and characterized by several techniques [13].

Pyrimidine azodyes are also very important, therefore their complexes were prepared and characterized [14–16] by analytical and spectral methods.

The metal complexes of azodyes derived from $\beta$-diketone were the subject of many investigations, especially with those of hydroxynaphthalene or salicylic acid [17, 18]. Many azo compounds find uses in pharmaceutical analysis [19, 20]. Also, the azo compounds and their complexes have been used in the stabilization of low valent metal redox state [21, 22] as well as in organic synthesis [23, 24]. Although a variety of systems has been employed for the synthesis of azodyes, there remains much scope for the design and development of new chromophores.

In this work we describe Fe(III), Co(II), Ni(II), and Cu(II) complexes of azodye compounds (Fig. 1) prepared by reaction of the azodyes with the metal salts in refluxing ethanol.

## Results and Discussion

Table 1 lists some analytical data for the azodyes and its metal complexes. The ligands are soluble in most common organic solvents such as *DMF*, *DMSO*, ethanol, and methanol whereas the complexes are insoluble in common organic solvents. The molar conductance values in *DMF* ($10^{-3}$ *M* solutions) are too low, hence the complexes can be regarded as non-electrolytes [25], which reflects the coordinated nature of the chloride ions in the Fe(III) complexes.

### *Thermal Analysis*

The thermal gravimetric analysis of the mononuclear and binuclear complexes **8**, **9**, **10**, **13**, **14**, and **16** were studied from ambient temperature up to 800°C. The stages of decomposition, temperature ranges, and decomposition products as well as found and calculated mass loss percentage of the metal complexes under investigation are shown as follows:

For mononuclear Ni(II) and Cu(II) complexes with ($H_4L_I$) **9** and **13**, the thermograms show that the weight losses within the temperature ranges 28–122.8°C (% mass loss found 12.9, calculated 13.1) and 30–102°C (% mass loss found 8.0,

**Table 1.** Magnetic and molar conductivity values

| No | Complex | Formula | $\mu_{eff}$ BM | $\Lambda$ $\Omega^{-1}$ cm$^2$ mol$^{-1}$ ($10^{-3}M$ in *DMF*) |
|---|---|---|---|---|
| | $H_4L_I$ | $C_{14}H_{10}N_2O_6$ 302 | – | – |
| | $H_4L_{II}$ | $C_{18}H_{12}N_2O_6$ 352 | – | – |
| **1** | $[FeH_2L_ICl3H_2O]2H_2O$ | $C_{14}H_{18}N_2O_{11}ClFe$ 481.34 | 5.7 | 9.1 |
| **2** | $[Fe_2L_ICl_26H_2O]4H_2O$ | $C_{14}H_{26}N_2O_{16}Cl_2Fe_2$ 585.8 | 4.8 | 11.2 |
| **3** | $[FeH_2L_{II}Cl3H_2O]3H_2O$ | $C_{18}H_{22}N_2O_{12}ClFe$ 549.84 | 5.9 | 14.7 |
| **4** | $[Fe_2L_{II}Cl_26H_2O]4H_2O$ | $C_{18}H_{28}N_2O_{15}Cl_2Fe_2$ 694.68 | 4.4 | 13.3 |
| **5** | $[CoH_2L_I4H_2O]2H_2O$ | $C_{14}H_{20}N_2O_{12}Co$ 466.93 | 4.3 | 10.4 |
| **6** | $[Co_2L_I8H_2O]3H_2O$ | $C_{14}H_{28}N_2O_{17}Co_2$ 613.86 | 4.7 | 15.1 |
| **7** | $[CoH_2L_{II}4H_2O]3H_2O$ | $C_{18}H_{24}N_2O_{13}Co$ 534.93 | 4.8 | 11.9 |
| **8** | $[Co_2L_{II}8H_2O]4H_2O$ | $C_{18}H_{32}N_2O_{18}Co_2$ 681.86 | 4.6 | 12.7 |
| **9** | $[NiH_2L_I2H_2O]H_2O$ | $C_{14}H_{14}N_2O_9Ni$ 412.7 | d[a] | 11.4 |
| **10** | $[Ni_2L_I4H_2O]2H_2O$ | $C_{14}H_{18}N_2O_{12}Ni_2$ 523.4 | d | 13.8 |
| **11** | $[NiH_2L_{II}2H_2O]2H_2O$ | $C_{18}H_{18}N_2O_{10}Ni$ 480.7 | d | 15.2 |
| **12** | $[Ni_2L_{II}4H_2O]2H_2O$ | $C_{18}H_{20}N_2O_{12}Ni_2$ 573.4 | d | 9.1 |
| **13** | $[CuH_2L_I2H_2O]2H_2O$ | $C_{14}H_{16}N_2O_{10}Cu$ 435.5 | 1.8 | 11.7 |
| **14** | $[Cu_2L_I4H_2O]2H_2O$ | $C_{14}H_{18}N_2O_{12}Cu_2$ 533.04 | 1.8 | 12.3 |
| **15** | $[CuH_2L_{II}2H_2O]2H_2O$ | $C_{18}H_{18}N_2O_{10}Cu$ 485.54 | 1.9 | 14.2 |
| **16** | $[Cu_2L_{II}4H_2O]3H_2O$ | $C_{18}H_{22}N_2O_{13}Cu_2$ 601.08 | 1.85 | 13.1 |

[a] d = diamagnetic

calculated 8.3) which are attributed to volatilization of one lattice water molecule followed by loss of the two coordinated water molecules for complex **9** and two lattice water molecules for complex **13** are associated with the endothermic peak at 112°C and the broad endothermic peak at 98°C in the *DTA* thermogram for complexes **9** and **13**, respectively. The removal of two coordinated water molecules takes place within the temperature range 102–185°C (% mass loss found 8.1, calculated 8.3) with an endothermic peak at 121°C for complex **13**. The

temperature range 122.8–345°C (% mass loss found 33.8, calculated 33.4) is attributed to loss of salicylic acid associated with an exothermic peak at 218°C for complex **9** and the loss of a $N_2$ molecule within the temperature range 345–412°C (% mass loss found 6.5, calculated 6.8) with the exothermic peak at 378°C. Thermogram for complex **13** shows that the weight loss at the temperature range 185–390°C (% mass loss found 37.6, calculated 38.1) is due to loss of salicylic acid followed by loss of a $N_2$ molecule in one step with a broad exothermic peak at 285°C. The temperature ranges 412–695°C (% mass loss found 46.9, calculated 47.2) and 390–760°C (% mass loss found 46.1, calculated 45.8) associated with broad exothermic peaks at 527°C and 476°C represent the decomposition of the remainder ligand molecule leading to NiO for complex **9** and CuO for complex **13**.

The thermal gravimetric analysis of the binuclear Co(II) and Cu(II) complexes **8** and **16** with $H_4L_{II}$ show that the temperature ranges 30–115°C (% mass loss found 10.7, calculated 10.5) and 30–142°C (% mass loss found 8.7, calculated 9.0) display the volatilization of four and three water molecules associated with endothermic peaks at 112°C and 115°C in the *DTA* thermogram. The temperature ranges 115–320°C (% mass loss found 21.1, calculated 21.1) and 142–272°C (% mass loss found 12.5, calculated 12.0) are attributed to loss of eight and four coordinated water molecules with endothermic peaks at 183°C and 214°C for complexes **8** and **16**. The removal of a $N_2$ molecule takes place at 320–380°C (% mass loss found 4.0, calculated 4.1) and 272–333°C (% mass loss found 4.3, calculated 4.6) associated with exothermic peaks at 368°C and 385°C. The final stage of pyrolysis in the temperature ranges 380–785°C (% mass loss found 64.7, calculated 64.3) and 333–778°C (% mass loss found 74.6, calculated 74.5) is the decomposition of the metal complexes leading to CoO and NiO with broad exothermic peaks at 590°C and 562°C for complexes **8** and **16**, respectively.

The thermograms of binuclear Ni(II) and Cu(II) complexes of $H_4L_I$ **10** and **14** show that the temperature ranges 30–81.5°C (% mass loss found 7.1, calculated 6.8) and 30–135°C (% mass loss found 6.9, calculated 6.7) are attributed to volatilization of two lattice water molecules associated with endothermic peaks at 71°C and 95°C for complexes **10** and **14**, respectively. The four coordinated water molecules are eliminated for both complexes **10** and **14** within the temperature ranges 81.5–263°C (% mass loss found 13.9, calculated 13.7) and 135–258°C (% mass loss found 13.2, calculated 13.5) confirmed with endothermic peaks at 164°C and 183°C in DTA thermograms. The weight loss of temperature ranges 263–344°C (% mass loss found 5.6, calculated 5.3) and 258–327°C (% mass loss found 5.1, calculated 5.2) is due to the removal of a $N_2$ molecule. This step is confirmed with exothermic peaks at 285°C and 305°C for complexes **10** and **14**. The last step of decomposition lies within the ranges 344–765°C (% mass loss found 73.6, calculated 74.4) and 327–750°C (% mass loss found 75.1, calculated 74.8) associated with exothermic peaks at 498°C and 536°C for complexes **10** and **14**, corresponding to the decomposition of the remainder ligand leading to NiO and CuO for complexes **10** and **14**.

Based on the data gained from thermal analysis, the decomposition of mononuclear and binuclear complexes **9** and **10** as an example can be represented as shown in Schemes 1 and 2.

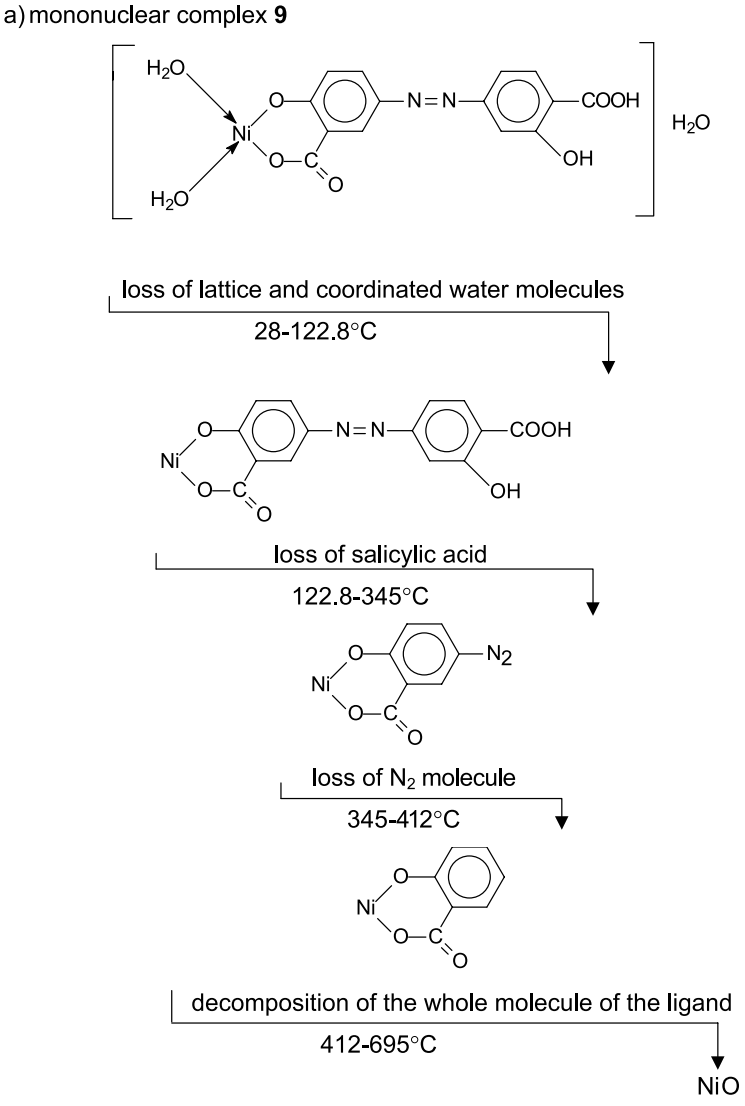


**Scheme 1**

*IR Spectra*

In order to ascertain the mode of bonding of the azodyes to the metal ions, the IR spectra of the free azodyes were compared with those of its metal complexes (Table 2). The bands due to the $\upsilon_{N=N}$ of the free azodyes $H_4L_I$ and $H_4L_{II}$ at 1420 and 1425 $cm^{-1}$ were observed at nearly the same position indicating non-coordination of the azo N-atoms. The phenolic C–O stretching vibrations appeared at slightly higher values (1231–1244 $cm^{-1}$) than that observed for the free ligands, confirming the alternative coordination through the phenolic oxygen atom [26]. For the acid moiety the bands of the carboxylic group were observed in the regions 1563–1624 and 1387–1396 $cm^{-1}$ arising from asymmetric [$\upsilon_{asy}(COO^-)$] and symmetric [$\upsilon_{sym}(COO^-)$] stretching modes of this group. This indicates the contribution of

b) binuclear complex **10**

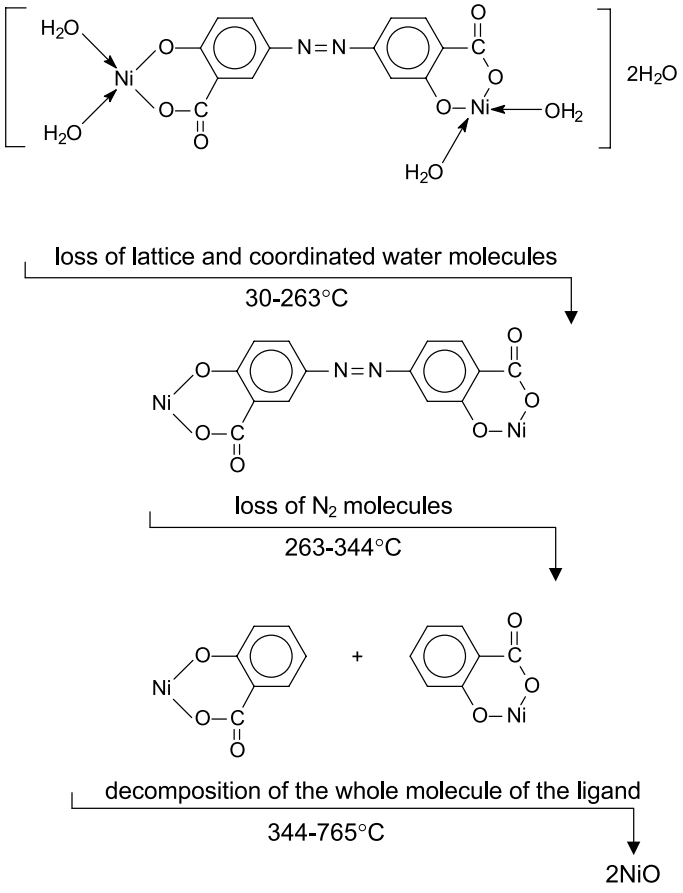


**Scheme 2**

the carboxyl group to the metal ion in the metal complexes. The difference between the asymmetric and symmetric stretching frequencies of the carboxylic group lies in the 176–228 $cm^{-1}$ range indicating the monobasic monodentate nature of the carboxyl group, hence exhibiting a free carbonyl group [27]. The bands due to the OH-groups at 3200–3350 ($\upsilon_{OH}$) and 1260–1280 ($\delta_{OH}$) $cm^{-1}$, display on obvious decrease in their intensity for the mononuclear complexes and they disappeared completely from the spectra of the binuclear ones. This behaviour is explained on the basis that the metal ion replaces two protons from the molecule. In the spectra of the complexes, the new bands in the range 455–483 $cm^{-1}$ can be assigned to the $\upsilon_{M-O}$ modes [28]. The IR spectra of all complexes show broad bands within the ranges 3399–3435, 760–786, and 583–625 $cm^{-1}$. These bands may by assigned to $\upsilon_{OH}$ stretching, rocking, and wagging modes of coordinated water molecules [29].

The above results indicate that the azodyes behave as dibasic bidentate ligands towards the metal ion in mononuclear complexes and as tetrabasic tetradentate ones towards the two metal ions for the binuclear ones.

**Table 2.** IR, electronic absorption spectra, and $g_{eff}$ values of complexes

| No | IR ($cm^{-1}$) | | | | | Electronic spectra ($cm^{-1}$) | $g_{eff}$ |
|---|---|---|---|---|---|---|---|
| | $\upsilon_{OH}$ | $\upsilon_{C-O}$ | $\upsilon_{sym(COO^-)}$ | $\upsilon_{asym(COO^-)}$ | $\upsilon_{M-O}$ | | |
| **1** | 3300 | 1233 | 1580 | 1390 | 460 | 21276 | 2.1986 |
| **2** | 3250 | 1238 | 1565 | 1392 | 466 | 20000 | 2.1454 |
| **3** | 3300 | 1233 | 1590 | 1392 | 455 | 202408 | 2.1856 |
| **4** | 3200 | 1240 | 1578 | 1386 | 478 | 18858 | 2.1246 |
| **5** | 3300 | 1238 | 1595 | 1388 | 455 | 14786, 22960 | 2.0295 |
| **6** | 3250 | 1237 | 1590 | 1390 | 455 | 14890, 22727 | 2.1394 |
| **7** | 3220 | 1242 | 1620 | 1390 | 474 | 15200, 22480 | 2.1480 |
| **8** | 3150 | 1234 | 1615 | 1392 | 465 | 14706, 23145 | 2.0678 |
| **9** | 3400 | 1236 | 1610 | 1388 | 482 | 21860 | – |
| **10** | 3300 | 1242 | 1615 | 1390 | 475 | 22398 | – |
| **11** | 3300 | 1234 | 1605 | 1392 | 482 | 21472 | – |
| **12** | 3250 | 1244 | 1595 | 1396 | 470 | 22368 | – |
| **13** | 3270 | 1236 | 1585 | 1386 | 464 | 16667, 20402 | 2.0925 |
| **14** | 3150 | 1246 | 1595 | 1390 | 460 | 17680, 21204 | 2.1290 |
| **15** | 3300 | 1238 | 1615 | 1392 | 475 | 17980, 22048 | 2.1420 |
| **16** | 3200 | 1234 | 1624 | 1394 | 480 | 18486, 21964 | 2.0210 |

*Magnetic Measurement and Electronic Absorption Spectra*

The magnetic moments, Table 1, of the mononuclear Fe(III) complexes **1** and **3** are 5.7 and 5.9 BM per Fe atom. These values are consistent with the acceptable values (5.92 BM) for the high spin Fe(III) ion ($S = 5/2$) [30]. The magnetic moment values for binuclear Fe(III) complexes **2** and **4** are 4.8 and 4.4 BM per Fe atom, respectively, which is lower than that corresponding to the spin only value for five unpaired electrons of a high spin $d^5$ system in octahedral structure. This is presumably caused by spin–spin coupling due to the existence of metal–metal interaction between the iron atoms in the crystal lattice of the binuclear complexes. The metal–metal interaction would occur between two Fe(III) ions from different molecules [31]. The electronic spectra, as nujol mull, Table 2, of the Fe(III) complexes show one band at 18858–21278 $cm^{-1}$ which can be assigned to $^6A_{1g} \rightarrow {}^4T_{2g}$ transition, characteristic of octahedral geometry [32].

The values of magnetic moments of the Co(II) complexes **5**–**8** are 4.3–4.8 BM, respectively, lying within the range reported for octahedral Co(II) [33]. The electronic spectra of the Co(II) complexes consist of two bands at 14706–15200 and 22480–23145 $cm^{-1}$ which can be assigned to $^4T_{1g} \rightarrow {}^4A_{2g}$ (F) and $^4T_{1g} \rightarrow {}^4T_{1g}$ (P) transitions, respectively, confirming the octahedral stereochemistry of the complexes [34, 35].

The mononuclear and binuclear Ni(II) complexes **9**–**12** are diamagnetic and their electronic spectra show one band at 21472–22472 $cm^{-1}$ which can be assigned to $^1A_{1g} \rightarrow {}^1B_{1g}$ transition [36] with the Ni(II) present in square planar environment.

The Cu(II) complexes **13–16** have a magnetic moment of 1.65–1.8 BM corresponding to one unpaired electron [37]. The electronic transition spectra display two bands at 16667–18486 and 20402–22048 $cm^{-1}$ which can be assigned to $^2B_{1g} \rightarrow {}^2E_g$ transition and charge transfer band, respectively, confirming square planar geometry around Cu(II).

*ESR Spectra*

X-band ESR spectra of the mononuclear and binuclear Fe(III), Co(II), and Cu(II) complexes were measured in the solid state at 300 K in order to gain knowledge about the geometries around these metal ions. The $g_{eff}$ values are depicted in Table 2.

The ESR spectra of mononuclear Fe(III) complexes **1** and **3** exhibit intense sharp signals showing the sixtet fine structure characteristic of high spin $d^5$ Fe(III) in octahedral environment [38]. For binuclear complexes **2** and **4** the spectra show some broadening and the fine structure tends to be blurred due to iron–iron interaction. This is further confirmed from the $g_{eff}$-values being lower for the binuclear complexes than in the case of mononuclear ones. For mononuclear Co(II) complexes **5** and **7**, the ESR spectra (Fig. 2) show the normal broadened signals with no hyperfine structure characteristic of Co(II) high spin octahedral structure [39]. The ESR spectra of mononuclear and binuclear Cu(II) complexes **13–16** give broad signals with no hyperfine structure and the *g*-values indicate that Cu(II) complexes have square planar geometry around the Cu(II) ion.

The more positive contribution in the $g_{eff}$ values of the complexes under investigation than the value of a free electron (2.0023) indicates the covalent nature of bonding between the metal ion and ligand molecules [40].

Based on the results obtained above, the structures of the metal chelates can be represented as shown in Scheme 3.

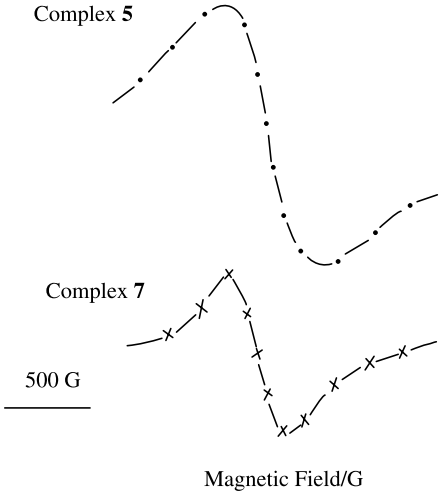


**Fig. 2.** X-Band ESR spectra of mononuclear Co(II) complexes **5** and **7**

a) mononuclear complexes

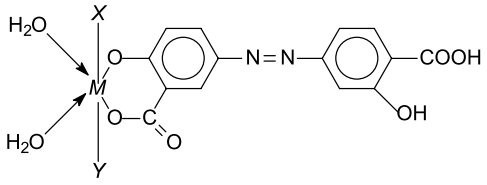


*X* and *Y* are absent for *M*=Ni(II) or Cu(II), *X*=*Y*=$H_2O$ for Co(II), and *X*=$H_2O$, *Y*=Cl for *M*=Fe(III)

b) homobinuclear complexes

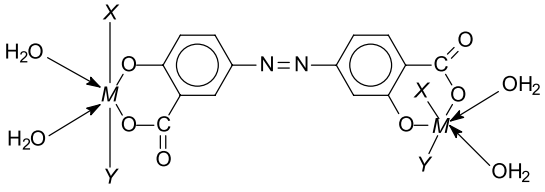


*X* and *Y* are absent for *M*=Ni(II) or Cu(II), *X*=*Y*=$H_2O$ for *M*=Co(II), and *X*=$H_2O$, *Y*=Cl for *M*=Fe(III)

**Scheme 3**

*Catalytic Activity*

The kinetics and mechanism of the oxidation of *N*,*N*,*N*′,*N*′-tetramethyl-*p*-phenylenediamine dihydrochloride (*TMPPD*) catalysed by mononuclear and binuclear copper complexes (**13** and **14**) were studied to check the activity of these copper complexes for this reaction. It has been reported [41, 42] that the *N*-substituted *PPD*s (*TMPPD*) undergo oxidation in two steps each comprising a single electron transfer (Scheme 4).

It is known that *p*-semiquinonediimine, *S*+, is the first oxidation product of a *N*-substituted *PPD*, *R* [43–45]. Fig. 3 shows time resolved spectra for the reaction of

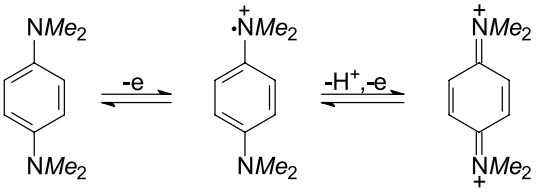


or in a simple way

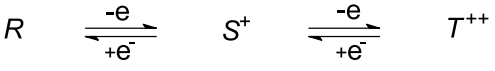


**Scheme 4**

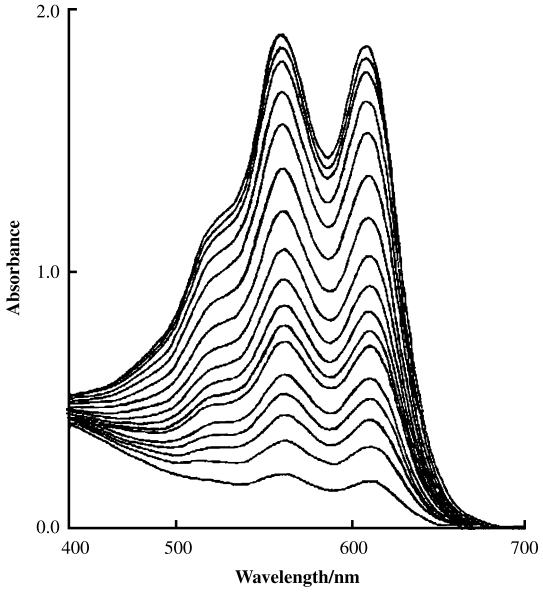


**Fig. 3.** Time resolved spectra for the reaction between $1\times10^{-4}$ *M* mononuclear Cu(II) complex **13** with $1\times10^{-4}$ *M TMPPD*

complex **13** with *TMPPD*. *N*,*N*,*N*′,*N*′-Tetramethyl-*p*-semiquinonediimine exhibits two bands at 612 and 565 nm, whereas, with complex **14** it exhibits two bands at 613 and 565 nm. Therefore, the formation rate for *p*-semiquinonediimine can easily be followed at 565 nm. At this wavelength, the measured absorbance is directly proportional to the change in concentration of the corresponding *p*-semiquinonediimine [46], Fig. 4. In addition to the two step oxidation according to Eqs. (1) and (2),

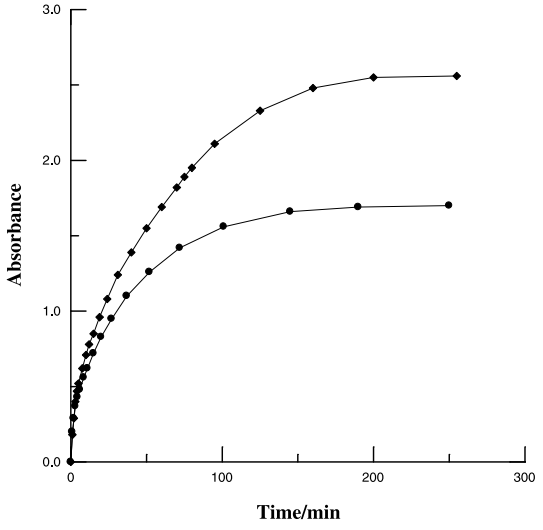


**Fig. 4.** Formation of *p*-semiquinonediimine after mixing $1\times10^{-4}$ *M TMPPD* with $1\times10^{-4}$ *M* mononuclear Cu-complex **13** (◆) and $1\times10^{-4}$ *M* binuclear Cu-complex **14** (●), respectively

a synproportionation takes place between the reduced and the totally oxidized form, as shown in Eq. 3 [43, 44].

$$[\mathrm{Cu^{II}}\text{-complex}] + R \xrightarrow{k_1} S^+ + [\mathrm{Cu^{I}}\text{-complex}] \tag{1}$$

$$S^+ + [\mathrm{Cu^{II}}\text{-complex}] \xrightarrow{k_2} T^+ + [\mathrm{Cu^{I}}\text{-complex}] + \mathrm{H^+} \tag{2}$$

$$R + T^+ + \mathrm{H^+} \underset{k_{-3}}{\overset{k_3}{\rightleftharpoons}} 2S^+ \tag{3}$$

The relative values of $k_3$ and $k_{-3}$ were found to be strongly dependent on the substituents on the *p*-phenylenediamine [43, 44]. The irreversible formation rate of *p*-semiquinonediimine, $S^+$, is given by Eq. (4).

$$\mathrm{d}[S^+]/\mathrm{d}t = k[R][\mathrm{Cu^{II}}\text{-complex}] \tag{4}$$

The actual concentrations of both $R$ and the complex can be expressed by the difference between their initial concentrations and the actual concentration of *p*-semiquinonediimine, $S^+$, as given by Eq. (5).

$$[R] = [R]_\mathrm{o} - [S^+] \text{ and } [\mathrm{Cu^{II}}\text{-complex}] = [\mathrm{Cu^{II}}\text{-complex}]_\mathrm{o} - [S^+] \tag{5}$$

Substituting Eq. (5) into Eq. (4) results in Eq. (6).

$$\begin{aligned} \mathrm{d}[S^+]/\mathrm{d}t &= k([R]_\mathrm{o} - [S^+])([\mathrm{Cu^{II}}\text{-complex}]_\mathrm{o} - [S^+]) \\ \mathrm{d}[S^+]/\mathrm{d}t &= k[R]_\mathrm{o}[\mathrm{Cu^{II}}\text{-complex}]_\mathrm{o} - k[S^+]([R]_\mathrm{o} + [\mathrm{Cu^{II}}\text{-complex}]_\mathrm{o}) + k[S^+]^2 \end{aligned} \tag{6}$$

Since $A = \varepsilon_\mathrm{s}\ [S^+]$ and path length = 1 cm substitution gives Eq. (7).

$$\mathrm{d}A/\mathrm{d}t = k\varepsilon_\mathrm{s}[R]_\mathrm{o}[\mathrm{Cu^{II}}\text{-complex}]_\mathrm{o} - kA[S^+]([R]_\mathrm{o} + [\mathrm{Cu^{II}}\text{-complex}]_\mathrm{o}) + kA^2/\varepsilon_\mathrm{s} \tag{7}$$

The absorbance change, $\mathrm{d}A/\mathrm{d}t$, was obtained by means of a mirror ruler at several points of the measured absorbance-time curves. The plot of $\mathrm{d}A/\mathrm{d}t$ versus $A$ gives a straight line with negative slope. The initial absorbance change $\mathrm{d}A/\mathrm{d}t_\mathrm{o}$ was determined from the intercept at zero time, *i.e.* at $A = A_\mathrm{o}^\mathrm{c}$, where $A_\mathrm{o}^\mathrm{c}$ is the absorbance caused by the complex (Fig. 5). Therefore, Eq. (7) becomes Eq. (8).

$$\mathrm{d}A/\mathrm{d}t_\mathrm{o} = k\varepsilon_\mathrm{s}[R]_\mathrm{o}[\mathrm{Cu^{II}}\text{-complex}]_\mathrm{o} \tag{8}$$

This means that the reaction is first-order in respect to both amine and oxidant. By substituting in Eq. (8), the rate constant, $k$, was found to be $1.58\times10^{-4}\ \mathrm{M^{-1}\ s^{-1}}$ and $5.03\times10^{-4}\ \mathrm{M^{-1}\ s^{-1}}$ for complex **13** and complex **14**, respectively.

It is clear that the activity of the binuclear complex **14** is more than three times of that of the mononuclear complex **13**. This may be attributed to the increased number of catalysis centers, mainly the copper ions.

The redox potential values for the mononuclear Cu(II) complex **13** and the binuclear one **14** amount to −0.11 and −0.2 V *vs.* SCE whereas that of *N*,*N*,*N*′,*N*′-tetramethyl-*p*-phenylenediamine dihydrochloride (*TMPPD*) is 0.21 V *vs.* SCE [47]. These values reveal that the electron transfer from *TMPPD* according to Eq. (1) requires a lower energy in case of the binuclear complete than the mononuclear one. This was gathered from the values of the equilibrium constants

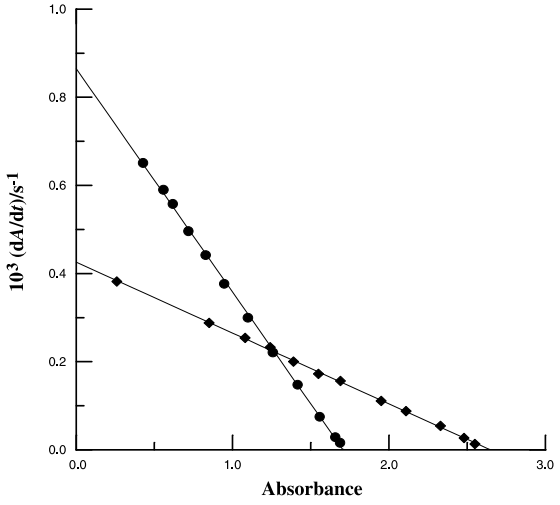


**Fig. 5.** Dependence of the formation rate of *p*-semiquinonediimine ($dA/dt$) on its corresponding concentration (measured as absorbance at 565 nm) according to Eq. (8) for the reaction of $1\times10^{-4}\,M$ Cu-complex **13** (◆) and $1\times10^{-4}\,M$ Cu-complex **14** (●), respectively, with $1\times10^{-4}\,M$ *TMPPD*

**Table 3.** Polarographic data obtained for some complexes in 0.1 *M* KCl at 25°C; values of $\alpha n_a$ and $\alpha$ were calculated from reciprocal slope ($S_1$) of the $\log(I/I_d - I) - E$ plots

| No | $I_d/\mu$A | | $-E_{1/2}$/V | | Slope ($S_1$)/mV | | $\alpha n_a$ | | $\alpha$ ($n_a = 2$) | |
|---|---|---|---|---|---|---|---|---|---|---|
| | (a) | (b) | (a) | (b) | (a) | (b) | (a) | (b) | (a) | (b) |
| $H_4L_I$ | 1.85 | – | 0.1 | – | 268.8 | – | 0.22 | – | 0.11 | – |
| **1** | 2.43 | 0.28 | 0.14 | 1.62 | 217.3 | 115.2 | 0.27 | 0.5 | 0.13 | 0.25 |
| **5** | 1.08 | 0.33 | 0.1 | 1.4 | 152.9 | 190.11 | 0.38 | 0.3 | 0.19 | 0.15 |
| **9** | 1.0 | 0.48 | 0.17 | 1.13 | 225.4 | 66.66 | 0.26 | 0.88 | 0.13 | 0.44 |
| **13** | 1.25 | 0.38 | 0.2 | 1.43 | 294.2 | 314.7 | 0.2 | 0.19 | 0.10 | 0.10 |
| **14** | 1.98 | 0.60 | 0.11 | 1.13 | 261.09 | 325.7 | 0.22 | 0.18 | 0.11 | 0.09 |
| **16** | 2.03 | 0.35 | 0.12 | 1.74 | 321.5 | 186.5 | 0.18 | 0.31 | 0.09 | 0.15 |

of the redox reaction determined from the potentials of the systems involved in the reaction using the relation $\log K = \left(\frac{E_{ox}-E_{red}}{0.059}\right)n$ where $E_{ox}$ is the potential of *TMPPD*, $E_{red}$ the potential of Cu(II) complexes **13** or **14** obtained from the DC polarographic waves (Table 3), and $n$ is the number of electrons involved in the reaction which equals unity.

The log $K$ values obtained amount to 5.424 and 6.949 for complexes **13** and **14**, respectively, which supports the higher reactivity of complexes **13** and **14**.

### *Electrochemical Studies*

The DC polarograms of the ligands display a single wave with $E_{1/2}$ at $-0.1$ V. This polarographic wave was attributed to the reduction of the azo center to the amine stage through the consumption of four electrons (Eq. (9)).

$$\text{Ar–N=N–Ar}^{\backslash} + 4e^- + 4H^+ \longrightarrow \text{Ar–NH}_2 + \text{H}_2\text{N–Ar}^{/} \qquad (9)$$

The electrode reaction proceeds in an irreversible manner as gathered from the analysis of the wave. The probable value of the transfer coefficient ($\alpha$), as calculated from the slope of the logarithmic analysis, amounts to 0.22 for $n_a = 1$. This reveals that the rate determining step in the electrode reaction involves one electron.

The cyclic voltammogram of the ligand gave a single 4-electrons irreversible peak ($E_p = 0.57$ V) which is in good accordance with those of the azo compounds having a similar structure investigated by *Eriksson et al.* [48].

The number of electrons involved in the overall reduction process of the azo center was found to equal 4, corresponding to its cleavage reduction to two amine derivatives which agrees well with the behaviour of similar compounds reported by *Eriksson et al*. [49].

The polarograms of the metal complexes **1**, **5**, **9**, **13**, **14**, and **16**, exhibit two waves, the first one is due to the reduction of the N=N group of the ligand whereas the more negative wave represents the reduction of the complexed metal ions. The $E_{1/2}$ values for the ligand and metal ions in the complexes lie at more negative potentials compared to those of the free ligand and the non complexed metal ions. Analysis of the waves due to the reduction of the metal ions and the ligand revealed that the electrode reaction proceeds in an irreversible manner. The most probable values of $\alpha$ and $n_a$ are given in Table 3. The height of the ligand wave is almost double that for the metal ion in case of the mononuclear complexes **1**, **5**, **9**, and **13** but both waves have equal heights with the binuclear ones **14** and **16**. Since the reduction of the metal ion involves the consumption of two electrons, then the reduction of the azo center would involve four electrons, supporting the results gained from the height of the wave of the free ligand (Table 3). It is worthy to mention that the reduction wave of $Cu^{2+}$ joins strongly the ligand wave.

The effect of Hg-height at mercury head indicated that the reduction waves are mainly controlled by diffusion with partial kinetic or adsorption contribution.

The cyclic voltammograms of the complexes were recorded in the region for the reduction of the metal ions only for the Co(II) and Ni(II) complexes **5**, **6**, and **9** (Fig. 6).

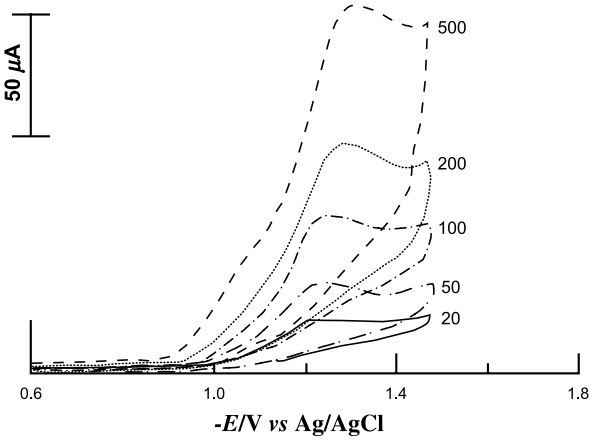


**Fig. 6.** Cyclic voltammograms of complex **5** at different scan rates

The CV gave single cathodic peaks but no anodic peaks were observed, which supports the irreversible nature of the electroreduction of the complexed metal ions. The peak potential $E_p$ shifts to more negative potential with scan rate whereas $i_p$ increases obviously. This behaviour supports the irreversible diffusion controlled behaviour of the electrode reaction. This trend finds further evidence from the linear plot of $E_p$ *vs.* $v^{1/2}$ and $i_p$ *vs.* $v$.

### *Biological Activity*

A primary study of the Minimum Inhibitor Concentrations (*MIC*) of the azo compounds and its complexes on *Gram* positive bacteria (*Staphylococcus aures* and *Bacillus subtilis*) and *Gram* negative bacteria (*Escherichia coli* and *Pseudomonos aeruginosa*) are recorded in Table 4.

From Table 4, it is clear that the *MIC* is much larger for metal complexes than for the ligand. Such increased activity of metal chelates can be explained on the basis of chelation theory [50]. Chelation considerably reduces the polarity of the metal ions because of partial sharing of its positive charge with the donor groups and increased $\pi$-electrons delocalization over the whole chelate ring. Such chelates could enhance the lipophilic character of the central metal atom. This increased lipophility leads to break down of the permeability barrier of the cell and thus retards the normal cell processes [51]. The general trend of *MIC* against *Gram* positive and *Gram* negative bacteria was found to lie in the order **15** > **14** > **13** > **3** > **1** > **7** > **5** > **10** > **9**.

The mononuclear and binuclear Cu(II) complexes have a relatively higher activity against *Gram* positive and *Gram* negative bacteria, whereas the mononuclear and binuclear Ni(II) complexes have the lowest activity.

**Table 4.** Minimum Inhibator Concentration ($\mu g/cm^3$) of azo compounds and complexes against *Gram* positive and *Gram* negative bacteria

| Organism / Compound | *Gram* positive bacteria | | *Gram* negative bacteria | |
|---|---|---|---|---|
| | *B-su* | *St-aur* | *E-coli* | *Ps-aur* |
| $H_4L_I$ | 200 | 250 | 150 | 200 |
| $H_4L_{II}$ | 250 | 150 | 200 | 250 |
| **1** | 100 | 50 | 100 | 100 |
| **3** | 100 | 3.1 | 50 | 100 |
| **5** | 150 | 150 | 100 | 200 |
| **7** | 150 | 100 | 100 | 150 |
| **9** | 200 | 150 | 200 | 150 |
| **10** | 150 | 200 | 100 | 150 |
| **13** | 3.1 | 100 | 3.1 | 50 |
| **14** | 50 | 3.1 | 50 | 3.1 |
| **15** | 3.1 | 3.1 | 50 | 3.1 |

## Experimental

The chemicals used for preparing the azodyes and the metal complexes were of reagent grade from BDH. The azodyes were prepared by coupling the diazonium salt of 4-aminosalicylic acid with salicylic acid or 1-hydroxy-2-naphthoic acid in alkaline solution following the known procedure [52]. The products were recrystallised from ethanol and the purity of the azodyes was confirmed by constancy of melting points and IR spectra. A solution of metal chloride (1 or 2 mmol) in ethanol was added to a hot solution of the azodyes (1 mmol) in the same solvent. The complex started to form after reflux for 2 h. After cooling, the precipitated complex was filtered off, washed with hot ethanol several times, dried in vacuo over $P_4O_{10}$, and then stored in a desiccator over $CaCl_2$.

Elemental analyses (C, H and N) were performed at the central microanalytical laboratory, Cairo and Tanta Universities; their results agreed favourably with the calculated values. The metal contents were determined by *EDTA* complexometric titration [53] and atomic absorption technique. IR spectra were recorded on a Perkin Elmer 1430 infrared spectrometer as KBr pellets. The electronic absorption spectra of the solid complexes were obtained on a Shimadzu 240 UV-Vis spectrophotometer using the Nujol mull method. Magnetic susceptibilities were determined on a Johnson Matthey magnetic susceptibility balance at room temperature (25°C) using $Hg[Co(SCN)_4]$ as calibrant. Diamagnetic corrections were calculated from *Pascal*'s constants. The ESR spectra were measured on Joel-X-band model JES $FE_2$ XG spectrometer equipped with an E-101 microwave bridge. The thermal studies (TGA and DTA) were achieved using a Shimadzu TG 50 thermal analyzer.

Kinetic measurements were carried out on a Shimadzu 240 UV-Vis spectrophotometer. The optical path length was 1 cm and the course of the reaction was followed at 565 nm which is the wavelength of maximum absorbance of the corresponding *p*-semiquinonediimine formed from *TMPPD*. The solutions of *TMPPD* and the oxidants were prepared immediately before being used. Stock solutions were prepared with doubly distilled water purged with $N_2$ gas for *ca.* 30 min. The metal complexes' solutions were prepared in $DMF/H_2O$ (50% $v/v$).

The pen recording polarograph Sargent-Welch model 4001 was used for studying the polarographic behavior of the azo compounds and their metal ion complexes under investigation. The cell described by *Meites* [54] was used for recording the polargramms at a dropping mercury electrode (DME) ($m = 1.03\,\mathrm{mgs}^{-1}$, $t = 3.3$ s, and mercury height $h = 60$ cm) and a saturated calmol electrode (SCE) as a reference electrode, supplied by Sargent-Welch.

The cyclic voltammogramms of the complexes under investigation were recorded using a potentiostate model 264 A (PAR-from EG&G). The 303A electrode assembly, supplied by EG&G, with a hanging mercury drop electrode (area $= 2.6 \times 10^{-2}\,\mathrm{cm}^2$) as a working electrode, a Pt wire as a counter electrode, and $Ag/AgCl/KCl_s$ as reference electrode was used.

The nutrient agar solid medium contained *per* $1000\,\mathrm{cm}^3$ ($pH = 7.2$): beef extract 3 g, peptone 5 g, nail 5 g, and agar 20 g. It was sterilized in high pressure steam for 30 min, serial dilutions of the azodyes and its complexes were prepared containing $250\,\mu\mathrm{g/cm}^3$ down to $3\,\mu\mathrm{g/cm}^3$. The bacteria used for testing the biological activity of the ligands and their complexes were *Gram* positive bacteria (*Staphylococcus aures* and *Bacillus subtilis*) and *Gram* negative bacteria (*Escherichia coli* and *Pseudomonos aeruginosa*) provided by the biology department. It was found that these bacteria exhibit obvious sensitivity towards organic and organometallic compounds.

## References

[1] Pfitzner H (1972) Angew Chem **11**: 312 (Eng)
[2] Shama SA (1996) Egypt J Anal Chem **5**: 13
[3] Konovalov LV, MaslenneKova IS, Shemyakin VN (1971) Zh Neorg Khim **16**: 2872 (Russ) C A 148564 K
[4] Adam FA, El-Haty MT, Amrallah AH, Abdalla NA (1988) Bull Soc Chim Fr **4**: 605

[5] Abdel-Latif SA, Hassib HB (2002) J Therm Anal Calar **68**: 983
[6] Kandil SS, Abdel-Hay FI, Issa RM (2001) J Therm Anal Cal **63**: 173
[7] El-Saied FA, Ayad MI, Issa RM, Aly SA (2000) Polish J Chem **74**: 919; (2001) **75**: 941
[8] Misra TK, Das D, Shinha C, Ghosh PK, Pal CK (1998) J Inorg Chem **37**: 1972
[9] Byabartta P *et al.* (2002) J Coord Chem **55**: 479
[10] Dinda J, Pal S, Ghosh BK, Cheng J, Liao FL, Lu TH, Sinha C (2002) J Coord Chem **55**: 1271
[11] Mohamed GG, Zayed MA, EL-Gamel NEA (2002) Spectrochimica Acta **58**: 3167
[12] Sengupta S, Chakraborty I, Chakravorty A (2003) Eur J Inorg Chem 1157 and references therein
[13] Sherif OE *et al.* (2003) J Therm Anal Cal **74**: 181 and references therein
[14] Santra PK, Das D, Misira TK, Roy R, Sinha C, Peng SM (1999) Polyhedron **19**: 1909
[15] Roy R, Santra PK, Das D, Sinha C (2002) Synth React Inorg Met Org Chem **30**: 1975
[16] Senapoti S, Ray US, Santra PK, Sinha C, Slawin AMZ, Derek J (2002) Polyhedron **21**: 753
[17] El-Baradie KY, Issa RM, Gaber M (2004) Indian J Chem **43**(A): 1126
[18] Amin AS, Moustafa MM, Issa RM (1997) Talanta **44**: 311
[19] Karpinska J, Kulikowska M (2002) J Pharm Biomed Anal **29**: 153
[20] Issa YM, Amin AS (1996) Mikrochim Acta **124**: 203
[21] Wong WY, Cheung SH, Lee SM, Leung SY (2000) J Organomet Chem **36**: 596
[22] Pramanik K, Shivakumar M, Ghosh P, Chakravorty A (2000) J Inorg Chem **39**: 195
[23] Santra PK *et al.* (2002) Europ J Inorg Chem 1124
[24] Ghosh AK *et al.* (1999) Organometallic **18**: 5086
[25] Geary W (1971) J Coord Chem Rev **7**: 81
[26] Viswanathamurthi P, Natarajan K (1999) Transition Met Chemistry **24**: 638
[27] Robinson SD, Uttley MF (1973) J Chem Soc Dalton Trans 1912
[28] Ferraro JR (1971) Low Frequency Vibration of Inorganic and Coordination Compounds. Plenum Press, New York
[29] Nakamoto K (1970) IR spectra of Inorganic and Coordination Compounds. Wiley, New York
[30] Hay MT, Hainaut BJ, Geib SJ (2003) Inorg Chem Commun **6**: 431
[31] Syamal A, Kale KS (1982) Indian J Chem (A) **21**: 439
[32] Srivastava PC (1973) J Inorg Nucl Chem **35**: 3613
[33] Lever ABP, Levis J, Nyholm RS (1962) J Chem Soc 1235
[34] Carlin RL (1968) Trans Metal Chem **1**: 3
[35] Jorgenson CK (1962) J Inorg Nucl Chem **24**: 1521
[36] Lever ABP (1984) Inorganic Electronic Spectroscopy. Elsevier, Amsterdam, p 452
[37] Sacconi L (1966) Coord Chem Rev **1**: 126
[38] Drago RS (1977) Physical Methods in Chemistry Saunders. Philadelphia, pp 481, 494
[39] Von Telewsky A, Fievz H (1973) Adv Chim Acta **56**: 977
[40] Fidone I, Stevens KWH (1959) Proc Phys Soc **73**: 116
[41] Mori I, Tominaga H, Fujita Y, Matsuo T (1997) Anal Lett **30**: 2433
[42] Mori I, Tominaga H, Fujita Y, Matsuo T (1997) Anal Lett **30**: 953
[43] Nickel U, Klein B, Hsin-min Ber Bunsenges J (1987) Phys Chem **91**: 997
[44] Nickel U, Haase E, Tharmann B (1991) Z Phys Chem **170**: 159
[45] Ibrahim A Salem, Mohamed Gaber, Diaa F Badr Eldeen (1999) Trans Met Chem **24**: 511
[46] Nickel U, Thormann B Fresenius (1990) J Anal Chem **336**: 316
[47] Allen J Bard, Larry R Faulkner (1980) Electrochemical Methods. Wiley, New York, p 702
[48] Eriksson Alf, Nyhlom Leif (1999) Electrochimica Acta **40**: 4029
[49] Eriksson Alf, Nyhlom Leif (2001) Electrochimica Acta **496**: 1113
[50] Srivastava RS (1981) Inorg Chim Acta **56**: 65
[51] Gupta N, Swaroop R, Singh RV (1997) Main Group Met Chem **14**: 387
[52] Gaber M, Hassanein M, Ahmed HA (1986) Indian J Tex Res **11**: 48
[53] Schwarzenbach G (1957) Complexometric Titration (Transl by H. Irving). Methuen, London
[54] Meites L (1965) Poloragraphic Techniques. Interscience, New York, p 240